Journal of Applied Polymer Science

Electrospun Polymeric Coatings on Aluminum Alloy as a Straightforward Approach for Corrosion Protection

Amin Firouzi, Costantino Del Gaudio, Francesca Romana Iamastra, Giampiero Montesperelli, Alessandra Bianco

Department of Enterprise Engineering, University of Rome—Tor Vergata, INSTM RU Tor Vergata, Viale del Politecnico, 00133 Rome, Italy

Correspondence to: A. Firouzi (E-mail: firouzi.amin@gmail.com)

ABSTRACT: Several metals and alloys are susceptible to corrosion attack and this usually implies the accurate selection of a specific material depending on the working conditions and the characteristics of the environment to which it will be exposed to. However, it could represent a restriction at the same time because a limited range of materials can be practically considered. In addition, they could be also characterized by unsuitable properties for the intended application and high costs. To address this issue, polymeric coatings exhibit high potentiality to be a valid alternative to toxic chromates, allowing to deal with the most appropriate metallic materials and affordable deposition procedures. In this work, polyvinyl alcohol (PVA) fibrous coating was successfully collected onto aluminum alloy-6082 by means of electrospinning technique. The anticorrosion performance of the final system has been evaluated in 3 wt % NaCl solution by means of electrochemical impedance spectroscopy (EIS). To avoid PVA disintegration in aqueous environment, several crosslinking procedures were assessed using glyoxal. The two most promising ones (120°C for 60 min and 150°C for 15 min) were then considered for a further investigation. Crosslinked PVA mats showed improved properties as compared to the as-spun case, as demonstrated by mechanical and thermal analyses. Electrochemical tests revealed that crosslinked coatings can protect aluminum substrates against corrosion, especially for the electrospun PVA coating treated at 120°C. In this case, after 270 h, a significant corrosion resistance of about 26 kΩ was recorded with respect to the blank alloy (about 3.8 kΩ). © 2014 Wiley Periodicals, Inc. J. Appl. Polym. Sci. **2015**, *132*, 41250.

KEYWORDS: biodegradable; coatings; electrochemistry; electrospinning; fibers

Received 19 March 2014; accepted 2 July 2014

DOI: 10.1002/app.41250

INTRODUCTION

Metallic materials are commonly used for a large number of industrial applications and innovative alloys have been developed in order to better fit the requirements for a specific use. However, the correct selection of these materials is strictly related to the environmental conditions and corrosion is the typical critical issue that has to be addressed for a safe and long lasting performance of metallic components. For this aim, different approaches based on anticorrosive coatings and corrosion inhibitors have been proposed, each of them being characterized by pros and cons. The presence of chromates, for instance, can rise concerns for the human health and environment.[1–4] In addition, the production costs of specific materials and the definition of *ad hoc* technological processes to overcome such a drawback represent a relevant limitation.

In this regard, a proposal, that could widen the restrictions above listed and give the possibility to deal with "common" materials (e.g., not specifically designed to be corrosion resistant) that can be properly combined for this aim, is therefore desirable. As a proof of concept, aluminum alloys can be a valuable class of material to be tested due to their large applications in several industrial fields. Unfortunately, aluminum alloys have unsatisfactory corrosion resistant features. In particular, they are subjected to pitting corrosion and this represents a limitation that, however, might be overcome collecting a polymeric layer onto the metallic surface as a protective coating, for instance. Not all the fabrication techniques are eligible since many of them require a polymeric solution in organic solvents that may alter the surface and represent a major source of environmental concern because they are volatile at normal temperatures and pressures.[1] A suitable alternative might be electrospinning, which allows to cover a metallic target with dry fine fibers. Briefly, electrospinning is a straightforward, cost-effective and versatile methodology for the production of nonwoven micro- and/or nanofibrous fabrics for, e.g., filter membranes, fuel cells,

composite reinforcement, sensors, drug delivery, tissue engineering.[5] The technical process requires the application of high voltage to a polymeric solution flowing through a capillary to generate an electrically charged jet. Increasing the voltage, the induced electrostatic field promotes the deformation of the polymeric drop, initially hold at the tip of the capillary, from hemispherical to conical, the so-called Taylor cone. When a critical value is attained, a polymeric jet is ejected from the tip of the Taylor cone toward a grounded target. Covering the capillary-to-target distance, the jet experiences instability phenomena that contribute to stretch and reduce fiber diameter. At the end of the process, the collected mat is generally made up of thin fibers randomly oriented.[6] Morphology of the electrospun fabrics depends on fluid properties (viscosity, conductivity, surface tension, and dielectric constant) and on operating parameters such as applied voltage, capillary-to-target distance, flow rate, jet current, and environmental conditions.[7]

Previous studies evaluated the role of collected electrospun mats onto metallic substrates as an effective means against corrosion. The influence of electrospinning and dip coating approaches were investigated and compared on the degradation of Mg alloy covered with poly(lactic acid), both techniques enhanced the corrosion resistance, the electrospinning giving a further improvement for prolonged immersion period.[8] Polyvinyl chloride fibers were electrospun onto aluminum, stainless steel, and brass substrates and the corrosion protective response was assessed in 3.5 wt % NaCl solutions, showing that the polymeric layer lowered the corrosion rates and shifted the corrosion potential toward the less negative potential for all the tested materials.[9] A diblock perfluoropolymer, i.e., poly-(heptadecafluorodecylacrylate-*co*-acrylic acid)-*b*-poly(acrylonitrile), was electrospun onto aluminum surfaces in order to provide superhydrophobicity and improved corrosion resistance.[10]

In this study, poly(vinyl alcohol) (PVA), a cheap polymer that can be easily processed by several fabrication techniques, was selected. It usually considered for different aims, including the development of miniature supercapacitors,[11] magnetic composite nanofibers,[12] tissue engineering,[13] or food packaging.[14] Being a water soluble polymer, PVA can be safely processed avoiding the use of organic solvents and thus limiting the possible exposure to toxic compounds. This could be a drawback at the same time, due to the intrinsic instability of the final product in the presence of water. However, this issue can be addressed by crosslinking the polymer chains in order to improve structural stability and mechanical properties. The most commonly used techniques to crosslink PVA involve dialdehydes, such as formaldehyde or glyoxal,[15–17] being di-functional and tetra-functional agents, respectively.[18]

The here proposed study presents a simple method, and the related assessment, to improve the resistance of metallic materials to corrosion, collecting crosslinked electropsun PVA fibrous layers onto aluminum alloy 6082 samples. The suitability of this approach was verified investigating a number of preliminary experimental conditions, and then selecting the most promising ones. A detailed analysis was carried out by means of scanning electron microscopy, differential scanning calorimetry (DSC), infrared spectroscopy, and mechanical characterization. Finally, the ability of PVA coatings to act as an effective protection against corrosion was evaluated for a prolonged time period performing EIS tests in 3 wt % NaCl solution.

MATERIALS AND METHODS

Metallic Substrate

The substrate material used for the current work was aluminum alloy 6082. Disks of 18 mm diameter and 1.5 mm thickness were polished using SiC grit papers. The grinded samples were washed in ethanol, rinsed in distilled water and finally dried in air at room temperature before to be used as collectors for the electrospun mats, as explained in the following sections.

Preparation of e-Spun Solutions

Aqueous PVA solutions were prepared by dissolving the PVA powder (99 + %hydrolyzed, $M_w = 130{,}000$ *Sigma-Aldrich*) in deionized water at 80–90°C, the resulting mixtures were kept under magnetic stirring for about 2–3 h. Four PVA aqueous solutions of different concentrations, i.e., 4, 6, 8, or 10 wt % were considered. After cooling to room temperature, in order to lower the surface tension of the solution, *Triton X-100* (*Sigma-Aldrich*), a nonionic surfactant, was added to each solution (1 wt % with respect to PVA). The obtained solutions were then stirred for 24 h at room temperature.

Crosslinked PVA mats were collected by adding glyoxal (40 wt % in H_2O (~8.8*M*), *Sigma-Aldrich*) (10 wt % with respect to PVA) to the polymeric solution to be electrospun. To keep the pH value in the range 2–3 (*pHmeter "334-B, Amel Instruments, Italy"*), phosphoric acid was also added. Solutions were ready for electrospining after 24 h under magnetic stirring at room temperature.

Deposition of the Fibrous Coating by Electrospinning

Fibrous polymeric coatings were directly electrospun onto aluminum alloy 6082 circular targets. In this article, the term "target" will refer to these AA6082 circular collector.

PVA solutions were poured in a glass syringe and electrospun in steady flow rate regime by means of a high voltage power supply (SL30, Spellman, USA) and a digitally controlled syringe pump (KD 130 Scientific, USA).

In the case of electrospun PVA mats containing glyoxal, samples were heated up in an oven in air to activate the crosslinking reaction.[18,19]

Different thermal treatments have been considered, as summarized in Table I.

Characterization of the e-Spun Solutions

All e-spun solutions were characterized in terms of viscosity and electrical conductivity. Viscosity measurements were performed at 30°C by means of a digital viscometer (Brookfield DV-II+, Middleboro, USA) equipped with SC4-21 spindle at 20 rpm. Electric conductivity was measured by a CDM230 meter (Radiometer Analytical, France) calibrated with a 0.01D KCl solution (1408 μS/cm) at 25°C. All the measurements were repeated three times.

Table I. The Thermal Treatments Used for the Activation of the Crosslinking Reaction

Label	Curing temperature (°C)	Curing time (min)
A		5
B		15
C	120	30
D		60
E		5
F		15
G	150	30
H		60

Microstructural Characterization

The surface morphology of the electrospun PVA mats was analyzed by scanning electron microscopy (SEM) (*LEO Supra 35*) after gold sputtering. The average fiber diameter was calculated by randomly selecting about 50 fibers from the acquired SEM micrographs (ImageJ, NIH).

Gel Fraction

Soxhlet extraction of the hydrogel with water (50°C) was used to determine the gel fraction, which is the insoluble content of crosslinked polymer. For this aim, the crosslinked electrospun mats were allowed to swell by immersion in distilled water for 2 h. Swollen hydrogels were then subjected to soxhlet extraction for 24 h and then dried under vacuum at 30°C until they dried completely. A gel fraction (Gel %) was calculated using the following formula[20]:

$$Gel(\%) = \frac{W_a}{W_b} \quad (1)$$

where W_b and W_a are the weight of dry samples before and after extraction.

Thermal Analysis

Melting temperature (T_m) and melting enthalpy (ΔH_m) were determined by DSC (Netzsch DSC 200PC, aluminum DSC pans), considering the first heating scan in the following conditions: N_2 atmosphere (65 mL/min), heating rate of 10°C/min, temperature range 20–265°C. The crystallinity degree of electrospun samples was calculated from the respective melting enthalpies (ΔH_m), as previously reported[21,22]:

$$X_c = \frac{\Delta H_m}{\Delta H_m^0} \cdot 100 \quad (2)$$

where ΔH_m^0 is the melting enthalpy of 100% crystalline PVA (138.6 J/g).[21,23]

ATR-FTIR Spectroscopy

Neat and crosslinked PVA mats were characterized by means of FTIR spectrometry by using an attenuated total reflection (ATR) accessory equipped with ZnSe prism (Nicolet 3700, Thermo Fisher Scientific Inc.). Spectra were acquired in the range 4000–400 cm^{-1}, 256 scans were performed for each specimen at a resolution of 4 cm^{-1}.

Mechanical Characterization

Uniaxial tensile tests were carried out on dog-bone specimens cut out from the electrospun mats, according to ASTM D 1708 (testing length 22.25 mm, width 4.8 mm). Sample thickness was measured applying a pressure of 10 g/cm^2 by means of a custom-made setup including a digital micrometer equipped with a 5 N load gauge (Imada, IL). Mechanical tests were performed at 1.2 mm/min up to rupture by means of a universal testing machine equipped with a 100 N load cell (Lloyd LRX). The tensile modulus (E), the stress at break (σ_{max}), and the strain at break (ε_f) were calculated considering the nominal cross-sectional area of the specimen. Four specimens were tested for each type of electrospun mat.

Corrosion Testing

Electrochemical impedance spectroscopy (EIS) measurements of bare and fibrous-coated samples were carried out by means of a 1260 Solartron Frequency Response Analyzer and a 1287 Solartron Electrochemical Interface in 3% NaCl solution at room temperature. An alternate signal, 10 mV in amplitude, was applied at the open circuit potential (OCP) in the frequency range $10^{-2} \times 10^5$ Hz. A three-electrode setup, consisting of a platinum counter electrode, a saturated Ag/AgCl reference electrode and the investigated sample (~1.5 cm^2) as a working electrode was used. Data were collected and analyzed by Zplot-Zview softwares (Scribner Associates Inc.). SEM analysis was also performed to examine the surface morphology of the coated samples after electrochemical test.

RESULTS AND DISCUSSION

Characterization of e-Spun Solutions

Viscosity and electrical conductivity of PVA (8 wt %) solutions prepared for electrospinning are summarized in Table II. The

Table II. Viscosity, Conductivity, and Electrospinning Parameters of the Selected Samples

Sample	Solution	Viscosity (mPa s)	Conductivity (mS/cm)	Voltage (kV)	Feed rate (mL/h)	TCD (cm)	T.T. after electrospinning
Neat PVA	PVA	1115	1.540 ± 0.016			12	–
As-spun PVA/glyoxal	PVA/glyoxal	1315	2.786 ± 0.012	12	0.4	13	–
D							120°C, 60 min
F							150°C, 15 min

TCD, tip to collector distance; T.T., thermal treatment.

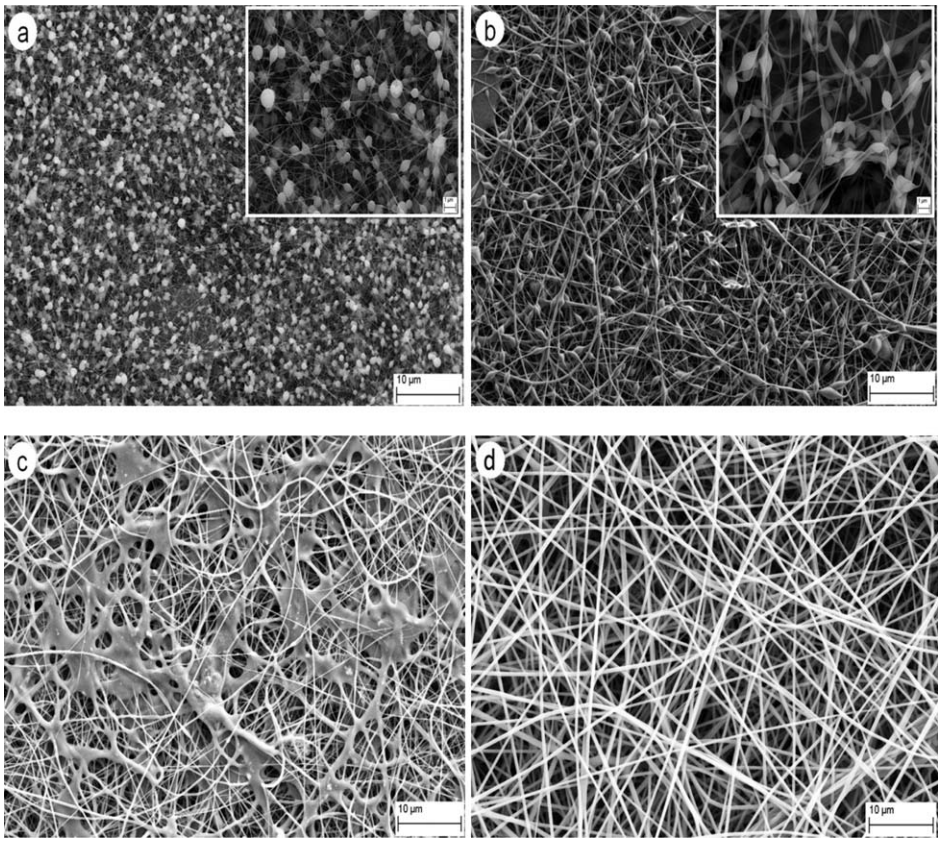

Figure 1. SEM micrographs of electrospun mats at (a) 4, (b) 6, (c) and (d) 8 wt % PVA solution. (a) at 12 kV, 14 cm, (b) at 12 kV, 10 cm, (c) at 16 kV, 14 cm, and (d) at 12 kV, 12 cm.

presence of glyoxal in the PVA solution resulted in increased viscosity from 1115 to 1315 mPa s, due to the enhancement of polymer chains entanglements,[19] and increased conductivity up to 2.786 ± 0.012 mS/cm.

As previously reported,[23] the surface tension of aqueous PVA solutions increases with the degree of hydrolysis of PVA. The initial incapability to electrospin 99+% hydrolyzed PVA water solution can be related to its high surface tension. To overcome this limitation, a small amount of nonionic surfactant, Triton X-100 (1 wt %), was used to lower the surface tension of the solution and facilitate the electrospinning of 99+% hydrolyzed PVA.[21]

Microstructure of Electrospun Mats

Characterization of Neat Electrospun PVA Mats. A series of experiments was performed to select the most suitable electrospinning conditions for the fabrication of uniform PVA fibers, including concentration, voltage, feed rate, and tip to collector distance (TCD). The electrospinning of 10 wt % PVA solution was not successful, the high viscosity resulting in formation of droplets at the needle tip. Figure 1 shows that the formation of beads progressively decreased by increasing the content of PVA from 4 to 8 wt %. Simultaneously, the shape of the beads changed from spherical to spindle-like until uniform fibers were collected starting from solution containing 8 wt % PVA.

However, not all the produced samples derived from 8 wt % PVA solutions showed a homogeneous microstructure. A crucial parameter in the electrospinning process is the applied voltage. Voltages lower than 10 kV were not high enough to reach the threshold value to start the process, causing the formation of solution droplets at the needle tip. On the other hand, applied voltages higher than 14 kV resulted in electrospinning along with electrospraying, the latter one becoming the main process. This condition also contributed to decrease the flight time of the fluid jet, leading to collect fused fibers on the target due to an incomplete solvent evaporation, even for samples electrospun at the maximum TCD of 14 cm [Figure 1(c)].[21,24]

The feed rate deeply affected the electrospinning process as well, preventing to collect suitable mats for high values (e.g., >0.7 mL/h). In the present work, lower feed rates (≤0.4 mL/h) were more desirable because formation of either droplets or wet fibers were prevented because of the enhancement of solvent evaporation process.[24] It has also been found that a proper target-to-needle distance is required to give the fibers enough time to dry before reaching the collector.[24,25] Hence, we observed that a TCD higher than 10 cm can be regarded a suitable working distance for the experimental protocol here proposed.[25]

Considering all the aforementioned variables, the optimal condition was obtained at 12 kV, 12 cm, and 0.4 mL/h, where a fine polymer jet was ejected from the tip of the needle and fibrous mats were deposited on the collector.

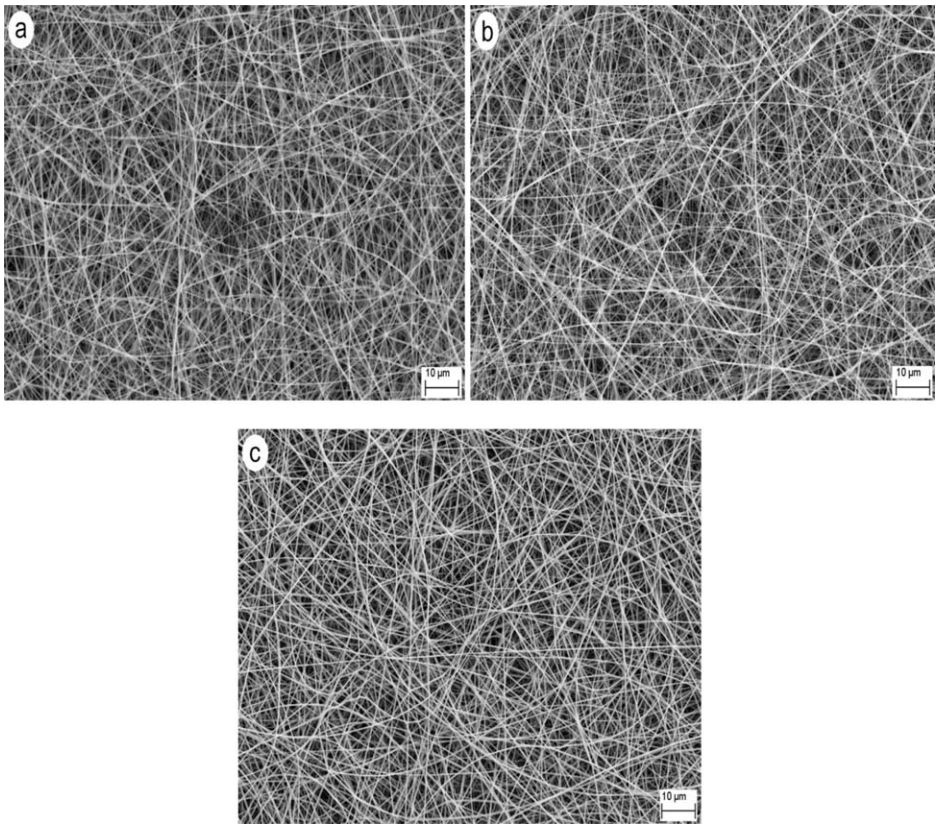

Figure 2. SEM micrographs of electrospun mats (a) as-spun PVA/glyoxal, (b) sample D and (c) sample F.

As it clearly results from SEM studies, in these conditions homogeneous PVA fibers free of defects were collected, the average diameter was 350 ± 60 nm [Figure 1(d)].

Characterization of Crosslinked Electrospun PVA Mats. Fibers free of defects were produced by electrospinning a 8 wt % PVA solution, containing 10 wt % of crosslinking agent. The optimal electrospinning conditions were 12 kV, 13 cm, and 0.4 mL/h. The average fiber diameter was 335 ± 50 nm, comparable to that measured for the neat PVA mats [Figure 2(a)].

To activate the crosslinking agent, curing process was necessary.[18] To investigate the influence of heat treatment, a series of thermal-treatment experiments was performed on as-spun PVA/glyoxal mats (Table I). Figure 3 shows an optical image of thermally treated samples after immersion in water for 10 days. Fibers were dissolved, either completely or partially, in the cases of A, B, C, and E, due to the short curing time that led to an inactivated or incomplete crosslinking reaction. Moreover, although samples G and H resisted against dissolution in water, fibrous mats became yellow and relatively brittle after thermal treatment due to thermal degradation and oxidation. This result was in good agreement with Ding et al.[18]

The variation of gel fraction versus crosslinking reaction time is presented in Figure 4. It can be clearly seen that for the curing temperature of 150°C, the shortest time at which about 100% gel fraction could be achieved corresponds to 15 min curing time (sample F) while that of the 120°C curing temperature was 60 min (sample D). In the case of 150°C curing temperature, in spite of the fact that longer time resulted in 100% gel fraction (i.e., G and H), samples have been degraded as previously mentioned. Also, sample F recorded relatively higher percent of gel fraction compared to that of the sample D.

SEM micrographs of properly crosslinked PVA mats (i.e., D and F), are shown in [Figure 2(b,c)]. The average fiber diameters were 310 ± 40 nm (D case) and 320 ± 50 nm (F case). The measured decrease in fiber diameter, even if not statistically significant, after thermal treatment could be related to intermolecular reactions causing crosslinking of fibrous mats. SEM images of samples D and F after 10 day immersion in water are also reported in [Figure 3(a,b)], respectively. The electrospinning and thermal treatment parameters of the optimum samples which were therefore used for the subsequent investigation are also summarized in Table II.

Differential Scanning Calorimetry

Melting temperature (T_m), melting enthalpy (ΔH_m) and crystallinity degree (X_c) of PVA granules and electrospun PVA mats were determined by DSC. The results are reported in Table III. The T_m values of the PVA granules and neat electrospun PVA were comparable, about 225 and 228°C, respectively.[18] As-spun PVA/glyoxal sample showed a significant decrease in the T_m and crystallinity degree compared to those of the former ones, being 212°C and 17%, respectively. As previously reported,[18,19] the activation of the crosslinking reaction resulted in a decreased crystallinity degree accompanied by the lowering of the melting temperature. Also, thermally treated PVA mats at 120°C (D)

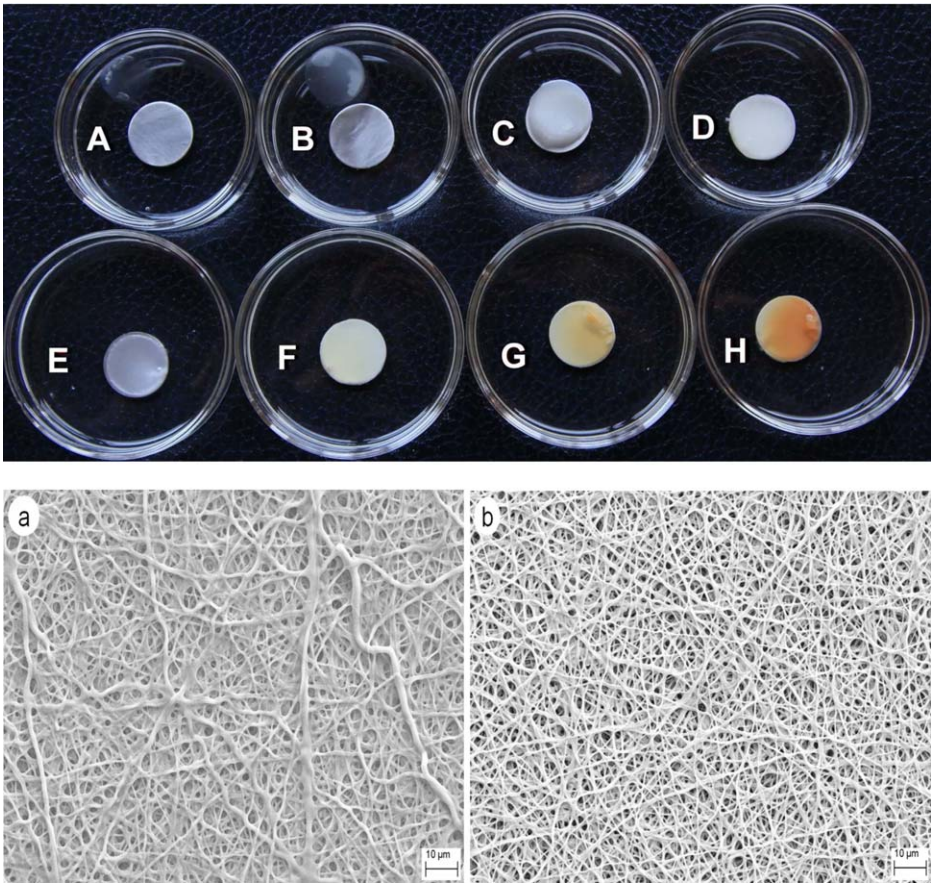

Figure 3. Digital image shows thermally treated samples A–H after 10 day immersion in water. SEM micrographs of (a) sample D and (b) sample F after 10 day immersion in water. [Color figure can be viewed in the online issue, which is available at wileyonlinelibrary.com.]

and 150°C (F) showed a significant difference in the crystallinity degree (ca. 12 and 20%, respectively). Previous studies have reported that the degree of crosslinking is inversely related to X_c, being directly related to glyoxal-PVA reaction time and temperature (i.e., 120°C for 60 min for sample D and 150°C for 15 min for sample F).[18,19]

Infra-Red Spectroscopy (ATR–FTIR) Analysis

Figure 5 shows the ATR–FTIR spectra for neat PVA, as-spun PVA/glyoxal and crosslinked PVA mats. All the investigated mats showed comparable spectra. As previously reported,[26] a broad band at about 3300 cm^{-1} can be referred to the hydroxyl groups. The asymmetrical and symmetrical C—H stretching are located at about 2940 and 2900 cm^{-1}, respectively. The secondary O—H in-plane bending and C—H wagging vibrations resulted at about 1420 and 1330 cm^{-1}. The C—C—C stretching band is presented at 1140 cm^{-1}, while the band at 1090 cm^{-1} represents the C—O stretching.

Mechanical Properties of Fibrous Mats

Mechanical properties of noncrosslinked and crosslinked electrospun mats as resulted from the uniaxial tensile tests are resumed in Table IV, stress–strain curves are shown in Figure 6. The tensile modulus and the stress at break were 53 ± 8 and 4.0 ± 0.4 MPa, respectively, for neat PVA mats. As-spun PVA/glyoxal mats exhibited similar tensile modulus and lower stress and strain at break, as compared to the former one. Reasonably, crosslinker molecules interacted with PVA polymeric chains leading to a different rearrangement during the

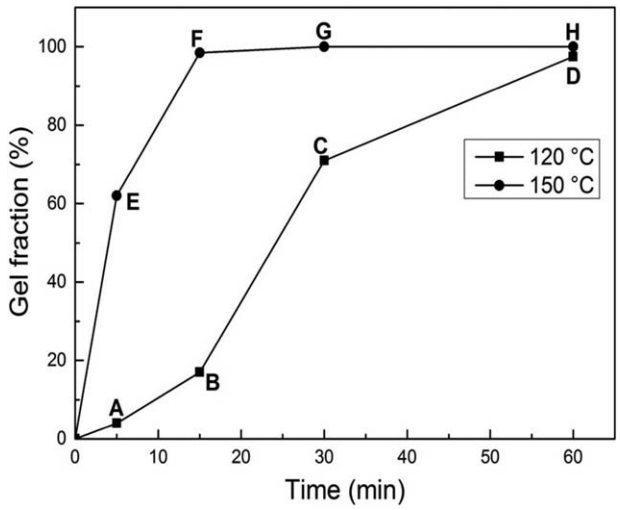

Figure 4. Variation of gel fraction of cross-linked PVA hydrogel versus crosslinking reaction time.

Table III. Thermal Properties of PVA Granules and Electrospun Mats

Sample	T_m (°C)	ΔH_m (J/g)	X_c (%)
Granules	225.1	64.82	46.77
Neat mat	228.6	59.36	42.83
As-spun PVA/glyoxal	212.4	23.06	16.64
D	196.4	16.68	12.03
F	202.3	27.95	20.16

Table IV. Tensile Modulus (E), Ultimate Tensile Stress (σ_{max}), and Strain at Break (ε_f) of PVA Electrospun Mats

Sample	E (MPa)	σ_{max} (MPa)	ε_f (%)
Neat mat	53 ± 8	4.0 ± 0.4	107 ± 12
As-spun PVA/glyoxal	50 ± 22	3.3 ± 0.2	91 ± 14
D	55 ± 5	4.6 ± 1.9	52 ± 10
F	65 ± 8	4.4 ± 1.5	38 ± 8

electrospinning process. This occurrence was in agreement with DSC analysis, evaluating a lower crystallinity degree, which in turn affected the final mechanical behavior of the tested mats.

Thermally treated electrospun mats (i.e., activated crosslinking reaction) showed higher mechanical properties, even if not statistically significant. The tensile moduli values were 55 ± 5 and 65 ± 8 MPa, whereas the stress at break were 4.6 ± 1.9 and 4.4 ± 1.5 MPa for D and F nonwoven fabrics, respectively. Moreover, strain at break of crosslinked mats assumed values significantly smaller than that measured on neat PVA mat, as can be expected. Crosslinking greatly affected the mechanical behavior of the electrospun mats, as verified by the remarkable modification of the resulting stress–strain curves. The polymer chains were tightly linked and slipping was hindered, leading to a stiffer structure. These results are in good agreement with previous studies.[18,27,28] According to Qiu and Netravali and Panzavolta et al.[27,29] crosslinking improves the mechanical properties, and in this study was also verified that an effective modification of the electrospun mat mechanical characteristics can be obtained at 150°C (Sample F).

EIS Assessment of Coating Systems

EIS is one of the most extensively used techniques capable to provide quantitative information on corrosion resistance of coating systems.[30–32] EIS measurements were carried out to estimate the evolution of barrier properties of crosslinked electrospun PVA coatings onto the Al-6082 alloy during immersion in 3 wt % NaCl corrosive media. The impedance at low frequency is a parameter, which can be used to compare corrosion protection performance of different coating systems being usually negligible the effect of the electrolyte resistance.[30,32]

Barrier Ability of Crosslinked Electrospun PVA Mats. It is well known that the EIS spectrum of a coated sample is given by the contribution of coating properties (Coating Capacitance C_{coat} and Pores Resistance R_{pore}) in the high frequency region (HF) and faradaic processes (Charge Transfer Resistance R_{ct} and Double Layer Capacitance C_{dl}) in the low frequency region.[33,34] In this research, the coating thickness is not an issue, but the impedance of the coating is the figure of merit. The analysis of frequency dependence of the complex impedance of the coated samples allows to evaluate the different components of the system. Corrosion protection capability was assessed by representing these components as a function of time.[32] The electrochemical response of sample D was evaluated in 3 wt % NaCl aqueous solution using EIS, as shown in Figure 7. EIS spectra of bare sample (not coated) is also reported for direct comparison. An increase of total resistance with respect to bare sample can be easily observed due to the barrier characteristics of the coating. The coated Al-6082 showed an initial high impedance of about 27 kΩ after 24 h of immersion. At this stage the water adsorption process begins, and the value of the coating capacitance increases with the uptake of water into the coating.[33] However, after 270 h of immersion, a significant corrosion

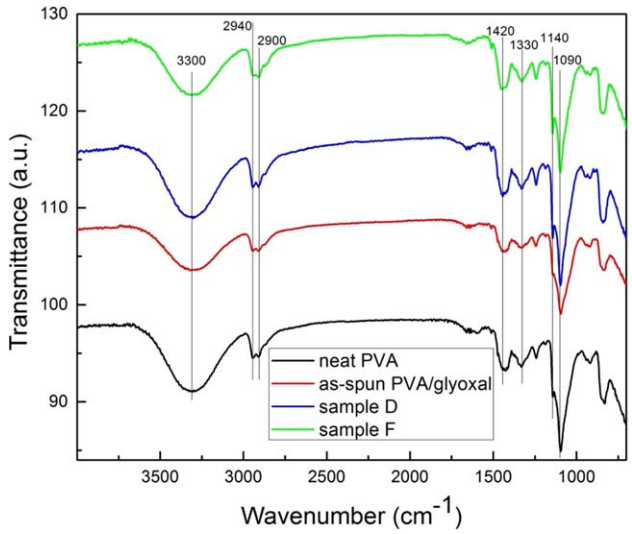

Figure 5. FTIR spectra of neat electrospun PVA, as-spun PVA/glyoxal, samples D and F. [Color figure can be viewed in the online issue, which is available at wileyonlinelibrary.com.]

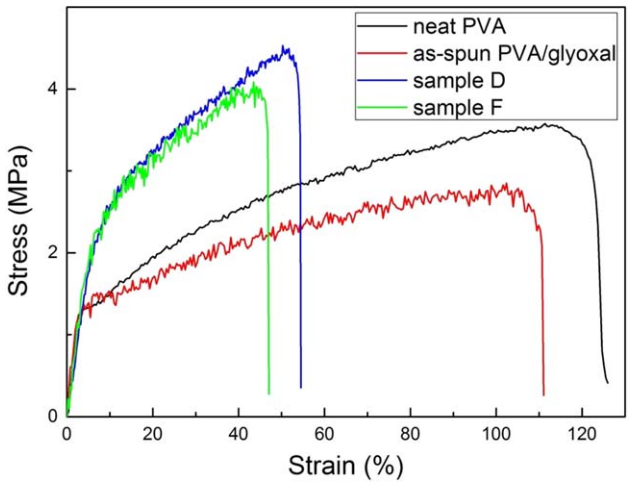

Figure 6. Typical stress–strain curves of neat electrospun PVA, as-spun PVA/glyoxal, samples D and F. [Color figure can be viewed in the online issue, which is available at wileyonlinelibrary.com.]

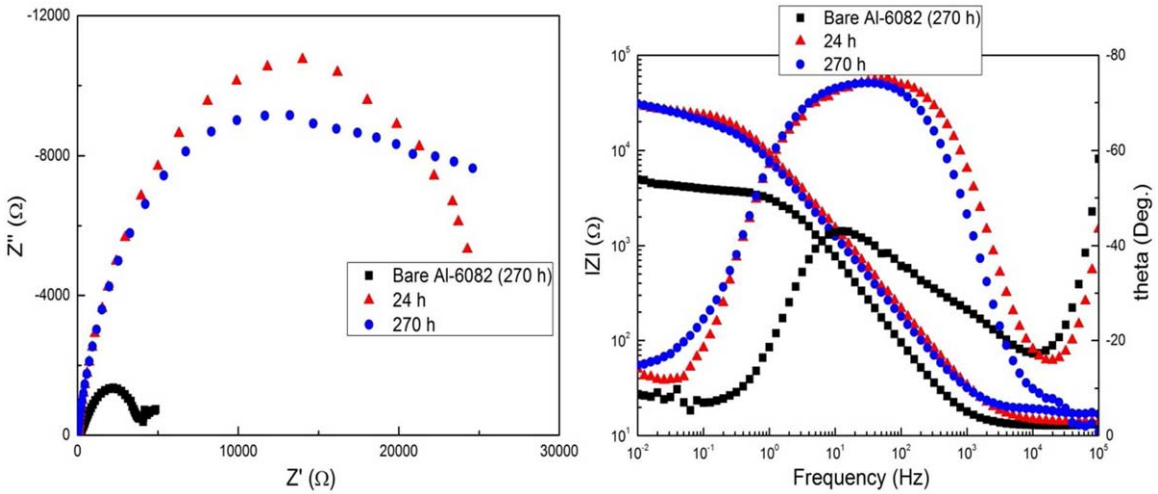

Figure 7. EIS spectrum of sample D in 3 wt % NaCl solution. [Color figure can be viewed in the online issue, which is available at wileyonlinelibrary.com.]

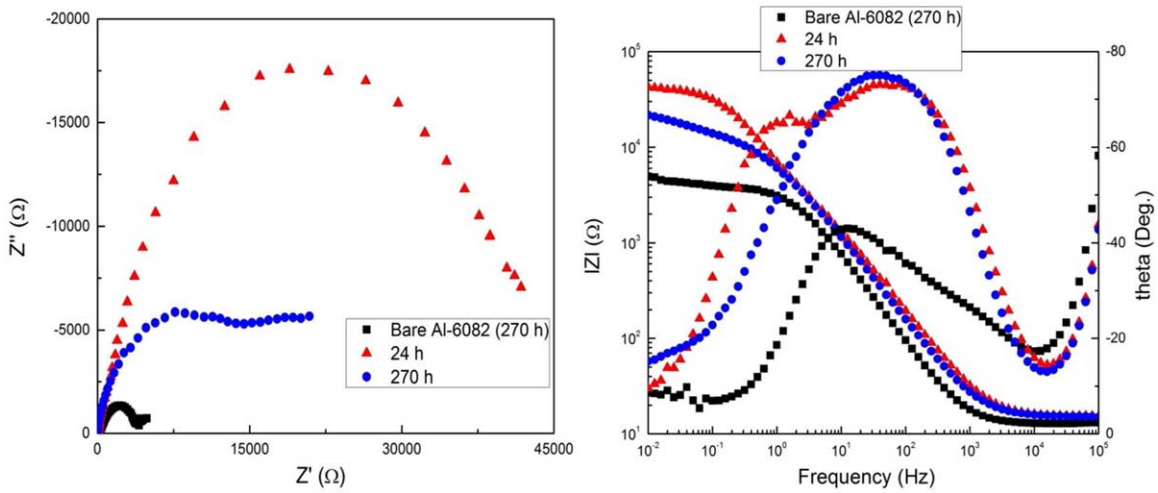

Figure 8. EIS spectrum of sample F in 3 wt % NaCl solution. [Color figure can be viewed in the online issue, which is available at wileyonlinelibrary.com.]

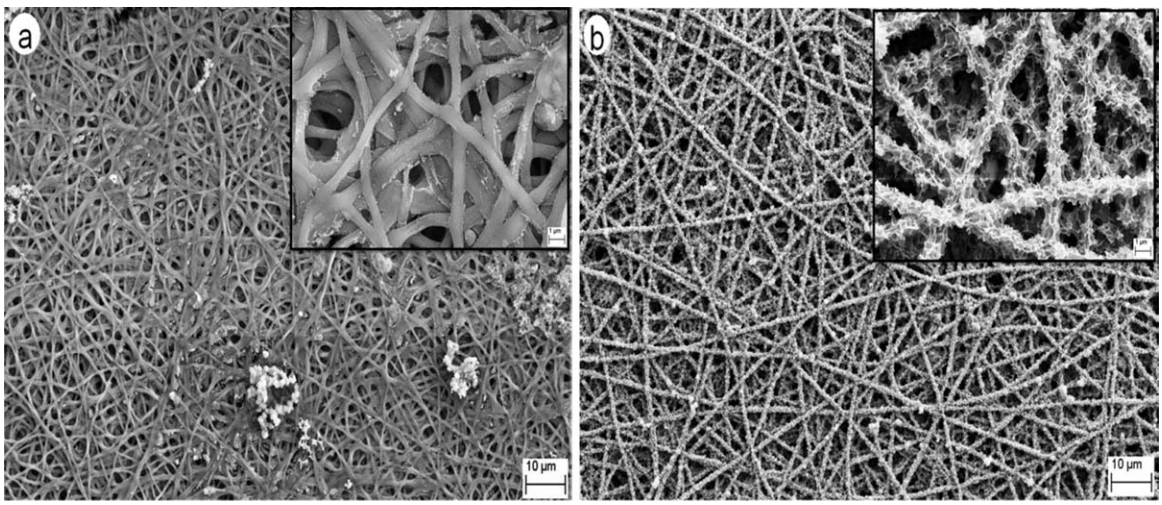

Figure 9. SEM micrographs of coating systems after electrochemical test, (a) sample D and (b) sample F.

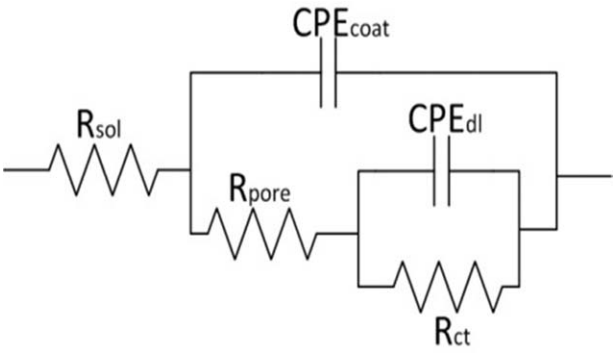

Figure 10. Representative equivalent circuit of electrospun coating systems used for the EIS data fitting.

resistance of about 26 kΩ was recorded whereas it was only 3.8 kΩ for the bare sample. Figure 8 reports the EIS spectra of the sample F in Nyquist and Bode representation. After 24 h of immersion in the electrolyte, the same corrosion behavior was observed (i.e., high resistance of about 45 kΩ). After 270 h of immersion, relatively lower impedance (about 14 kΩ) as compared to that of sample D, at 0.01 Hz frequency, was measured. The reason for this result may be due to the presence of larger voids within the fibrous mats in the sample F (Figure 9), as well as the fiber morphology seemed to be degraded after exposure to 3 wt % NaCl solution [inset magnification in Figure 9(b)], causing the electrolyte to reach the substrate and some faradaic process occurred.

For quantitative estimation of the corrosion protection performance of the coating systems in 3 wt % NaCl solution, experimental data were fitted using classical equivalent circuit models for intact coatings as shown in Figure 10.[34,35] This model was established assuming the following: R_{sol} was the resistance of the solution between working electrode and reference electrode. CPE_{coat} and R_{pore} referred to the capacitance and resistance of the electrospun fibrous coating, respectively. R_{ct} in parallel with CPE_{dl} represented the charge transfer resistance and double layer capacitance, respectively, originated from faradaic process present at the substrate/coating interface. Here, the constant phase elements (CPE) have been used instead of a real capacitance to take into account the nonideal behavior of the sample resulting from non-uniformity of the coatings.[30,36] Early exposure time to corrosive media hardly resulted in electrolyte penetrating through the pores of the coating. Thus, the electrospun mats exhibited high corrosion resistance. On extended immersion (up to 24 h), the coating was saturated and eventually, the electrolyte containing chloride ions reached the intermediate (substrate/coating interface) layer, which resulted in a decrease of resistance (R_{pore}). At this stage, the corrosion protection of the substrate is mainly attributed to the good barrier capability of the coating.[36] After 24 h of immersion, the film expanded the formation of the ionically conducting pathways and the electrolyte finally interacted with the substrate. The electrolyte diffusion rate through the film is determined by the density of the pores/defects in the coating.[36,37] Thus, the lower barrier properties of the sample F can be explained by two hypotheses: one is related to the chemistry of the coating (different thermal treatments, crosslinking degree, crystallinity), and another one can be related to a possible difference in the coating thickness, which is difficult to control during the electrospinning.[34] As an example, Figure 11 shows the fitting results obtained on the spectrum of the D and F coating systems after 270 h of immersion, in Bode representation, using the equivalent circuit of Figure 10. A perfect agreement between experimental and numerical data was obtained as χ^2 test values were lower than 10^{-4}, which means that the model could extract all the relevant information of the spectrum in the studied frequency range.

CONCLUSIONS

This study showed that a proper combination of a cheap polymer (PVA), a simple processing technique (the electrospinning) and a largely used metallic material in several industrial applications (aluminum) can provide a valuable system that can operate in corrosive environments. Electrospun PVA fibers free of defects were crosslinked following different routes, the two most promising ones were then fully characterized. Mechanical and

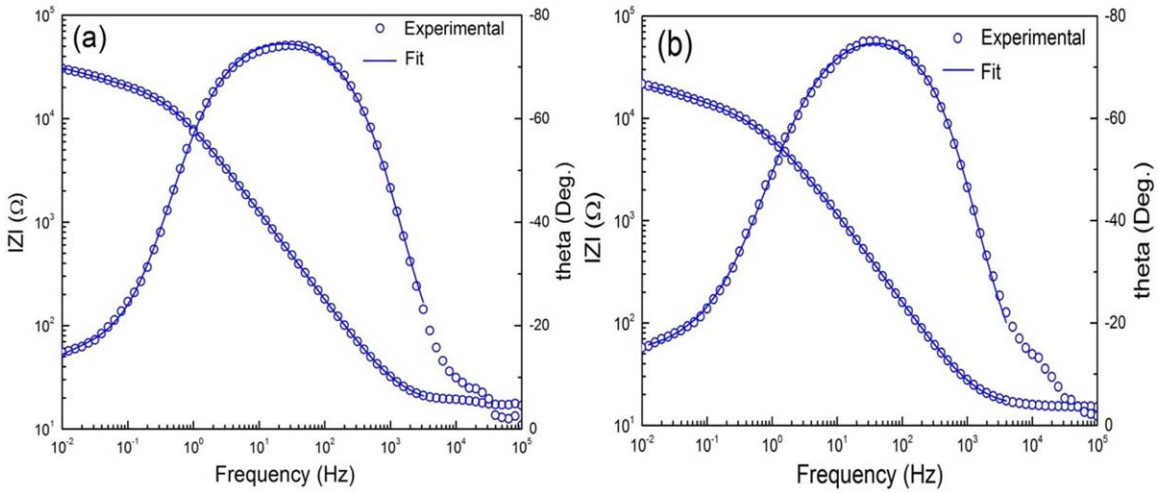

Figure 11. Comparison between EIS experimental data and curve fitting of (a) sample D and (b) sample F after 270 h immersion in 3 wt % NaCl solution in the Bode representation. [Color figure can be viewed in the online issue, which is available at wileyonlinelibrary.com.]

thermal assays confirmed the effectiveness of the chemical treatment, highlighting a clear improvement compared to the neat case. Most important, electrochemical measurements demonstrated the potential of the proposed coatings to prevent the corrosion of the aluminum substrate where electrospun PVA coating crosslinked at 120°C for 60 min recorded very high impedance of about 26 kΩ after a long immersion time (270 h) in 3 wt % NaCl environment. The acquired data clearly indicate that the here presented approach can be regarded either as (i) a cost-effective method to protect metallic materials and (ii) a platform to be further developed, acting not only as a protective layer, but also possible development of a new coating system with a self-healing functionality made of electrospun polymeric mats containing corrosion inhibitors.

REFERENCES

1. Sørensen, P. A.; Kiil, S.; Dam-Johansen, K.; Weinell, C. E. *J. Coat. Technol. Res.* **2009**, *6*, 135.
2. Raja, P. B.; Sethuraman, M. G. *Mater. Lett.* **2008**, *62*, 113.
3. Osborne, J. H.; Blohowiak, K. Y.; Taylor, S. R.; Hunter, C.; Bierwagon, G.; Carlson, B.; Bernard, D.; Donley, M. S. *Prog. Org. Coat.* **2001**, *41*, 217.
4. Twite, R. L.; Bierwagen, G. P. *Prog. Org. Coat.* **1998**, *33*, 91.
5. Ramakrishna, S.; Fujihara, K.; Teo, W.; Lim, T.; Ma, Z. An Introduction to Electrospinning and Nanofibers; World Scientific: Singapore, **2005**.
6. Frenot, A.; Chronakis, I. S. *Curr. Opin. Colloid Interface Sci.* **2003**, *8*, 64.
7. Lee, K. H.; Kim, H. Y.; Khil, M. S.; Ra, Y. M.; Lee, D. R. *Polymer.* **2003**, *44*, 1287.
8. Abdal-hay, A.; Barakat, N. A. M.; Lim, J. K. *Colloid Surf. A* **2013**, *420*, 37.
9. Es-saheb, M.; Elzatahry, A. A.; Sherif, E. S. M.; Alkaraki, A. S.; kenawy, E. R. *Int. J. Electrochem. Sci.* **2012**, *7*, 5962.
10. Grignard, B.; Vaillant, A.; De Coninck, J.; Piens, M.; Jonas, A. M.; Detrembleur, C.; Jerome, C. *Langmuir* **2011**, *27*, 335.
11. Jiang, L.; Vangari, M.; Pryor, T.; Xiao, Z.; Korivi, N. S. *Microelectron. Eng.* **2013**, *111*, 52.
12. Liu, F.; Ni, Q. Q.; Murakami, Y. *Text. Res. J.* **2013**, *83*, 510.
13. Asran, A. S.; Razghandi, K.; Aggarwal, N.; Michler, G. H.; Groth, T. *Biomacromolecules* **2010**, *11*, 3413.
14. Ge, L.; Zhao, Y. S.; Mo, T.; Li, J. R.; Li, P. *Food Control.* **2012**, *26*, 188.
15. Macho, V.; Fabíni, M.; Rusina, M.; Bobula, S.; Harustiak, M. *Polymer* **1994**, *35*, 5773.
16. McKenna, G. B.; Horkay, F. *Polymer* **1994**, *35*, 5737.
17. Kurihara, S.; Sakamaki, S.; Mogi, S.; Ogata, T.; Nonaka, T. *Polymer.* **1996**, *37*, 1123.
18. Ding, B.; Kim, H. Y.; Lee, S. C.; Shao, C. L.; Lee, D. R.; Park, S. J.; Kwag, G. B.; Choi, K. J. *J. Polym. Sci. Part B: Polym. Phys.* **2002**, *40*, 1261.
19. Blanes, M.; Gisbert, M. J.; Marco, B.; Bonet, M.; Gisbert, J.; Balart, R. *Text. Res. J.* **2010**, *80*, 1465.
20. Kumar, R.; Upadhyay, N. K.; Surekha, P.; Roy, P. K. *J. Appl. Polym. Sci.* **2009**, *111*, 1400.
21. Lamastra, F. R.; Bianco, A.; Meriggi, A.; Montesperelli, G.; Nanni, F. Gusmano, G. *Chem. Eng. J.* **2008**, *145*, 169.
22. Arbelaiz, A.; Fernández, B.; Valea, A.; Mondragon, I. *Carbohydr. Polym.* **2006**, *64*, 224.
23. Yao, L.; Haas, T. W.; Guiseppi-Elie, A.; Bowlin, G. L.; Simpson, D. G.; Wnek, G. E. *Chem. Mater.* **2003**, *15*, 1860.
24. Bhardwaj, N.; Kundu, S. C. *Biotechnol. Adv.* **2010**, *28*, 325.
25. Subbiah, T.; Bhat, G. S.; Tock, R. W.; Parameswaran, S.; Ramkumar, S. S. *J. Appl. Polym. Sci.* **2005**, *96*, 557.
26. Zhang, Y.; Zhu, P. C.; Edgren, D. *J. Polym. Res.* **2010**, *17*, 725.
27. Qiu, K.; Netravali, A. N. *Compos. Sci. Technol.* **2012**, *72*, 1588.
28. Zhang, L.; Chen, P.; Huang, J.; Yang, G.; Zheng, L. *J. Appl. Polym. Sci.* **2003**, *88*, 422.
29. Panzavolta, S.; Gioffrè, M.; Focarete, M. L.; Gualandi, C.; Foroni, L.; Bigi, A. *Acta Biomater.* **2011**, *7*, 1702.
30. Zhong, X.; Li, Q.; Hu, J.; Zhang, S.; Chen, B.; Xu, S.; Luo, F. *Electrochim. Acta.* **2010**, *55*, 2424.
31. Mehta, N. K.; Bogere, M. N. *Prog. Org. Coat.* **2009**, *64*, 419.
32. Lamaka, S. V.; Zheludkevich, M. L.; Yasakau, K. A.; Serra, R.; Poznyak, S. K.; Ferreira, M. G. S. *Prog. Org. Coat.* **2007**, *58*, 127.
33. Bagalà, P.; Lamastra, F. R.; Kaciulis, S.; Mezzi, A.; Montesperelli, G. *Surf. Coat. Technol.* **2012**, *206*, 4855.
34. Jorcin, J. B.; Scheltjens, G.; Van Ingelgem, Y.; Tourwé, E.; Van Assche, G.; De Graeve, I.; Van Mele, B.; Terryn, H.; Hubin, A. J. B. *Electrochim. Acta.* **2010**, *55*, 6195.
35. Bonora, P. L.; Deflorian, F.; Fedrizzi, L. *Electrochim. Acta.* **1996**, *41*, 1073.
36. Zhong, X.; Li, Q.; Hu, J.; Lu, Y. *Corros. Sci.* **2008**, *50*, 2304.
37. Wang, H.; Akid, R. *Corros. Sci.* **2007**, *49*, 4491.